Development of Kerr Electro-optic 3-d Electric Field Measuring Technique and its Experimental Verification

R. Shimizu, M. Matsuoka, K. Kato, N. Hayakawa, M. Hikita and H. Okubo

Department of Electrical Engineering, Nagoya University, Nagoya, Japan

ABSTRACT

We have developed a method to measure 3-dimensional electric field distributions in liquid dielectrics using the Kerr electro-optic effect combined with ac field modulation and circularly polarized light. We derived theoretical relations between an arbitrary electric field vector and a transmitted light intensity. The derived equations were verified by comparing the theoretical electric field profile with the experimental one in transformer oil with an axisymmetric electrode configuration, *i.e.* measured electric field vectors proved to agree well with theoretical ones. The light intensities experimentally obtained were transformed into axisymmetric electrode configuration by Abel transformation to calculate the electric field distribution.

1. INTRODUCTION

FOR highly reliable insulation design and diagnosis of electric power apparatus, it is indispensable to get information on electric field and space charge distributions in the field space. Especially under dc fields, space charge distorts the electric field distribution, and can result in fatal breakdown of the insulation. Hence, direct measurement of the electric field profile in dielectrics is highly desired.

The Kerr electro-optic field mapping technique is a direct measurement method of electric field distribution in liquid dielectrics. This technique allows us to measure the electric field profile with no disturbance. A number of reports on the direct electric field measurement using this technique have appeared. For instance, many researchers have performed highly sensitive measurements of electric field profiles in dielectric liquids with low Kerr constant, using a method combining electric field modulation and circularly polarized light incidence [1–5], when the electric field vector is perpendicular to the direction of light propagation. On the other hand, when the electric field vector is not perpendicular to the light propagation direction, some attempts are also made to measure the electric field profile in liquid with a parallel-plane electrode configuration and nonuniform field in axisymmetric electrode system [6–9]. However, there have been few reports on highly sensitive measurement of electric field vector with 3-dimensional components under nonuniform field configuration, and experimental investigation is not sufficiently done.

From the viewpoint mentioned above, this paper describes a new measurement technique with high sensitivity for seeking 3-dimensional electric field vectors; this technique utilizes Kerr electro-optic effect with a combined technique of ac electric field modulation and circularly polarized light. This method permits us to estimate the electric field strength and its direction from transmitted light intensity in an optical system. First, we derive a set of theoretical equations relating transmitted light intensity to the electric field vector. Second, we investigate experimentally the electric field distribution in transformer oil with an axisymmetric electrode configuration to verify the derived equations.

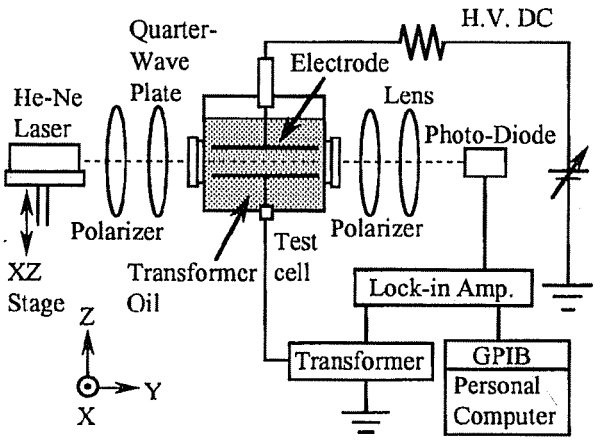

Figure 1. Experimental setup.

2. THEORETICAL RELATION BETWEEN ELECTRIC FIELD VECTOR AND TRANSMITTED LIGHT INTENSITY

2.1. MEASURING SYSTEM

Figure 1 illustrates the experimental setup for the measurement of electric field in transformer oil using the Kerr effect [2, 3]. Kerr constant $B = 3 \times 10^{-15}$ m/V^2 of transformer oil is so small that

1070–9878/96/ $3.00

we used a combined technique of ac electric field modulation and circularly polarized light to enhance the measuring sensitivity. As a light source, a He-Ne laser (7 mW, 632.8 nm) was used. The laser beam passes through a polarizer and a quarter-wave plate to get circularly polarized. After passing a test cell and an analyzer, the light is detected with a photodiode. The detected signal is taken to a lock-in amplifier synchronous with the modulation frequency ω and the second harmonic modulation frequency 2ω set in advance. In this measuring system, two ratios of the transmitted light intensities were obtained: (1) the ratio of the fundamental frequency component $I_{1\omega}$ to dc component I_{dc} and (2) the ratio of the second harmonic component $I_{2\omega}$ to I_{dc} of the transmitted light. Next, we will derive a set of equations to express the electric field vector from $I_{1\omega}/I_{dc}$ and $I_{2\omega}/I_{dc}$.

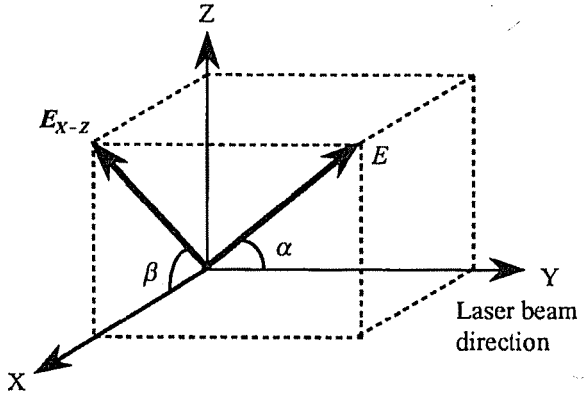

Figure 2. Electric field vector and laser beam.

2.2. TRANSMITTED LIGHT INTENSITY IN THE OPTICAL SYSTEM

Figure 2 shows the relationship between directions of an electric field vector and a laser beam. In this Figure, X, Z and Y axes represent horizontal, vertical, and laser beam propagation direction, respectively. α is the angle between Y axis and the electric field vector, and β is the angle between X axis and E_{X-Z}: the component of E cast on the $X-Z$ plane. In this paper, we assume the electric field strength is constant and $\alpha = 90°$; the electric field vector is perpendicular to the laser beam direction for axisymmetric electric field distribution.

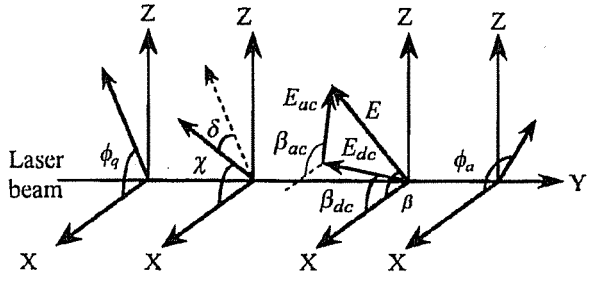

Figure 3. Optical arrangement.

Figure 3 shows the optical arrangement in the experimental set-up given in Figure 1. In Figure 3, we introduce the following four parameters ϕ_q, χ, δ and ϕ_a, concerning the optical arrangement. ϕ_q in the polarizer is the angle between transparent axis and X-direction. At the quarter-wave plate, we define two parameters χ and δ; χ represents the angle between the fast axis of the quarter-wave plate and the X-direction, and $\delta = \phi_q - \chi$. At the analyzer, ϕ_a is the angle between the transparent axis and X-direction. In the optical system without ac electric field modulation, the ratio of transmitted light intensity I_{out} to the intensity of input light I_{in}, is given by

$$\frac{I_{out}}{I_{in}} = \frac{1}{2} + \frac{1}{2}\cos 2\delta \cos 2(\chi - \phi_a) + \frac{1}{2}\sin 2\delta \sin 2(\beta - \phi_a)\Gamma \tag{1}$$

where Γ is the phase shift caused by the Kerr effect between two orthogonal components of an electric field wave propagating in a liquid dielectric with L in length. When applying electric field E_{X-Z}, Γ is given by

$$\Gamma = 2\pi B L E_{X-Z}^2 \tag{2}$$

where B is the Kerr constant. The B of transformer oil is small, $B = 3 \times 10^{-15}$ m/V^2, so that $\Gamma \ll 1$ at low electric fields, *e.g.* 10 kV/cm with $L = 10$ cm as in the present experimental conditions. Thus, in Equation(1), the following approximation is established: $\cos\Gamma \approx 1$, and $\sin\Gamma \approx \Gamma$.

When the ac electric field modulation is introduced in Equation (1), the electric field E_{X-Z} and the angle β are given by Equations (3) and (4), respectively,

$$|E_{X-Z}| = \left[(E_{dc}\sin\beta_{dc} + E_{ac}\cos\omega t \sin\beta_{ac})^2 + (E_{dc}\cos\beta_{dc} + E_{ac}\cos\omega t\cos\beta_{ac})^2\right]^{\frac{1}{2}} \tag{3}$$

$$\beta = \arctan\left[\frac{E_{dc}\sin\beta_{dc} + E_{ac}\cos\omega t\sin\beta_{ac}}{E_{dc}\cos\beta_{dc} + E_{ac}\cos\omega t\cos\beta_{ac}}\right] \tag{4}$$

At this point, we have four unknown parameters to solve for the two Equations (3) and (4): dc electric field strength E_{dc}, and its angle β_{dc} to the X-axis, ac electric field strength E_{ac} and its angle β_{ac} to the x axis.

Substituting Equations (3) and (4) into (1) and (2), one can derive the ratio of light intensity I_{out}/I_{in} as expressed by Equation (5).

$$\frac{I_{out}}{I_{in}} = \frac{I_{dc}}{I_{in}} + \frac{I_{1\omega}}{I_{in}}\cos\omega t + \frac{I_{2\omega}}{I_{in}}\cos 2\omega t \tag{5}$$

where

$$\frac{I_{dc}}{I_{in}} = \frac{1}{2}[1 + \cos 2\delta \cos 2(\chi - \phi_a)] + \pi BLE_{dc}^2 \sin 2\delta \sin 2(\beta_{dc} - \phi_a) + \frac{1}{2}\pi BLE_{ac}^2 \sin 2\delta \sin 2(\beta_{ac} - \phi_a) \quad (6)$$

$$\frac{I_{1\omega}}{I_{in}} = 2\pi BLE_{dc}E_{ac} \sin 2\delta \sin[(\beta_{dc} + \beta_{ac}) - 2\phi_a] \quad (7)$$

$$\frac{I_{2\omega}}{I_{in}} = \frac{1}{2}\pi BLE_{ac}^2 \sin 2\delta \sin 2(\beta_{ac} - \phi_a) \quad (8)$$

The second term of Equation (6) can be neglected because it is generally even smaller than its first term, *i.e.* $\pi BLE_{dc}^2 \ll 1$. Thus, measured ratios of light intensity $I_{1\omega}/I_{dc}$ and $I_{2\omega}/I_{dc}$ are given by

$$\frac{I_{1\omega}}{I_{dc}} = \frac{4\pi BLE_{dc}E_{ac} \sin 2\delta}{1 + \cos 2\delta \cos 2(\chi - \phi_a)} \sin[(\beta_{dc} + \beta_{ac}) - 2\phi_a] \quad (9)$$

$$\frac{I_{2\omega}}{I_{dc}} = \frac{\pi BLE_{ac}^2 \sin 2\delta}{1 + \cos 2\delta \cos 2(\chi - \phi_a)} \sin 2(\beta_{ac} - \phi_a) \quad (10)$$

2.3. EQUATIONS TO CALCULATE ELECTRIC FIELD VECTOR FROM TRANSMITTED LIGHT INTENSITY

Equations (3) and (4) are transformed into (9) and (10). Note that the Equations (9) and (10) can be obtained for a given angle ϕ_a, of the analyzer. Since there are only two equations for four unknown parameters to be obtained, we need two more equations. In order to get these additional equations, we measure the light intensities by changing the angle ϕ_a, of the analyzer. We can thus get four equations for two values of ϕ_a, and therefore solve the equations to obtain four unknowns. In the measurements, we rotated the analyzer by 45°, because both the ratios of the light intensity $I_{1\omega}/I_{dc}$ and $I_{2\omega}/I_{dc}$ are not zero [10].

Solving these four equations, the four unknown parameters are expressed as

$$E_{ac}^4 = \frac{4}{(2\pi BL)^2 \sin^2 2\delta}\left[\{1 + \cos 2\delta \cos 2(\chi - \phi_a)\}^2 (\frac{I_{2\omega}}{I_{dc}})^2 + \{1 - \cos 2\delta \sin 2(\chi - \phi_a)\}^2 (\frac{I_{2\omega}^{45}}{I_{dc}^{45}})^2\right] \quad (11)$$

$$\beta_{ac} = \tfrac{1}{2} \arctan\left[\frac{I_{2\omega}/I_{dc}}{I_{2\omega}^{45}/I_{dc}} \frac{1 + \cos 2\delta \cos 2(\chi - \phi_a)}{1 - \cos 2\delta \sin 2(\chi - \phi_a)}\right] + \phi_a \quad (12)$$

$$E_{dc}^2 = \frac{1}{4(2\pi BL)^2 E_{ac}^2 \sin^2 2\delta} \times [\{1 + \cos 2\delta \cos 2(\chi - \phi_a)\}^2 (I_{1\omega}/I_{dc})^2 + \{1 - \cos 2\delta \sin 2(\chi - \phi_a)\}^2 (I_{1\omega}^{45}/I_{dc}^{45})^2] \quad (13)$$

$$\beta_{dc} = \arctan\left[\frac{I_{1\omega}/I_{dc}}{I_{1\omega}^{45}/I_{dc}^{45}} \frac{1 + \cos 2\delta \cos 2(\chi - \phi_a)}{1 - \cos 2\delta \sin 2(\chi - \phi_a)}\right] + 2\phi_a - \beta_{ac} \quad (14)$$

where I_{dc}^{45}, $I_{1\omega}^{45}$ and $I_{2\omega}^{45}$ are dc, fundamental, and second harmonic components of transmitted light intensity with $\phi_a' = \phi_a - 45°$, respectively. From Equations (11) and (12), ac electric field vector components (E_{ac}, β_{ac}) are calculated with known parameters δ, χ, ϕ_a and measured $I_{2\omega}/I_{dc}$, $I_{2\omega}^{45}/I_{dc}^{45}$. Next, solving Equations (13) and (14) with the above obtained E_{ac}, β_{ac} one can readily calculate the dc electric field vector components (E_{dc}, β_{dc}).

As mentioned above, an electric field vector can be calculated from the measured transmitted light intensities. Note that the above procedure is applicable only for an arrangement in which the laser light travels through a Kerr cell while keeping the angle δ between the light propagation direction and the electric field vector at 90°, and the electric field strength is constant along the light path. When angle $\delta \neq 90°$, Equations (3) to (14) are valid if one replaces E_{dc} and E_{ac} with $E_{dc} \sin \alpha_{dc}$ and $E_{ac} \sin \alpha_{ac}$, respectively. In this case, all dc and ac electric field components can not be calculated with the above method alone. In such a case, Sumiyoshitani [6] derived formulas to obtain electric field components by measuring two ratios of the transmitted light intensities with rotation of the laser beam direction around the Z-axis. In other words, when the magnitude and direction of the electric field varies along the light path, some modification should be made; *e.g.* one has to combine the developed technique for computed tomography (CT) to solve 3-dimensional electric field distributions [9].

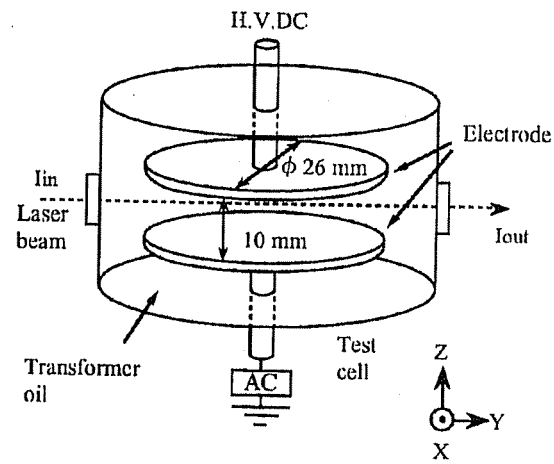

Figure 4. Axisymmetric parallel-plane electrode configuration in the test cell.

3. MEASUREMENT OF ELECTRIC FIELD DISTRIBUTION OF AXISYMMETRIC ELECTRODE CONFIGURATION

3.1. EXPERIMENTAL SETUP

In order to confirm the derived Equation (11) to (14) experimentally, we measured electric field distribution of an axisymmetric

electrode configuration illustrated in Figure 4. A pair of disk electrodes made of brass with diameter 26 mm for gap length 10 mm were placed in parallel in a stainless steel test cell filled with transformer oil. A dc voltage $V_{dc} = -10$ kV was applied to the HV electrode and an ac voltage $V_{ac} = 200V_{peak}$ with the frequency 1 kHz was superimposed on the grounded electrode. We detected the transmitted light intensity at the center position between two electrodes by scanning the laser beam in 1 mm steps in the X direction.

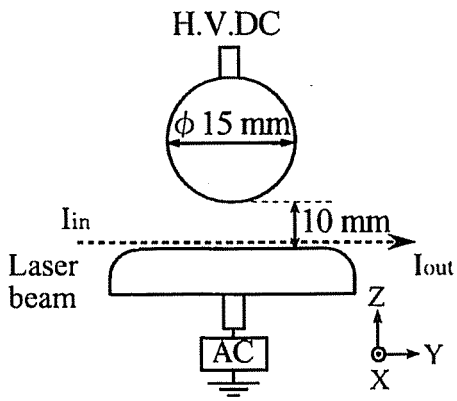

Figure 5. Axisymmetric sphere-plane electrode configuration.

Next, we replaced the upper plane electrode with a sphere electrode made of brass, 15 mm in diameter, illustrated in Figure 5. We measured the electric field distribution near the plane electrode after applying $V_{dc} = -10$ kV to the HV sphere electrode. Using Equations (11) to (14), we evaluated E_{dc}, E_{ac}, β_{dc} and β_{ac} from the measured $I_{1\omega}/I_{dc}$ and $I_{2\omega}/I_{dc}$. The oil was degassed with a vacuum pump, and then dry nitrogen gas was filled in the cell to atmospheric pressure. Volume resistivity ρ of the oil was kept at 10^{13} to 10^{14} Ωcm and moisture content was 10 to 20 ppm at room temperature. In order to measure the electric field profile at a steady state, measurements started 1 h after dc voltage application.

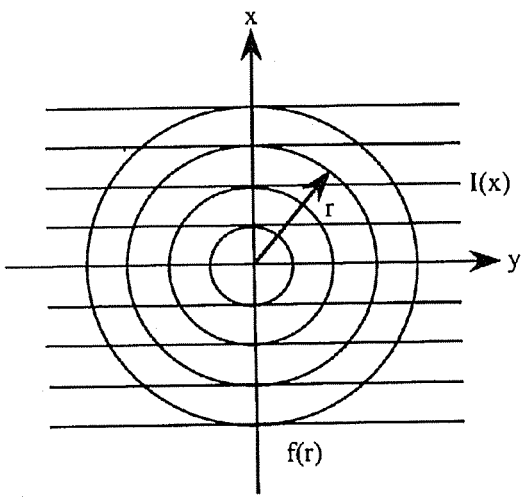

Figure 6. Abel transformation.

3.2. ABEL TRANSFORMATION

Since axisymmetric electrode configurations are used, we need to perform Abel transformation on the measured data to estimate the magnitude and angle of the electric field vector. In this Section, we briefly show the principle of Abel transformation. Let us suppose a physical value $f(r)$ having a rotational symmetry, that is, $f(r)$ depends only on the radius r. Let us also define $I(x)$ as the measured value along the path parallel to the Y axis for a given $f(r)$ as depicted in Figure 6. Then, the relationship between $f(r)$ and $I(x)$ is given by

$$f(r) = -\frac{1}{\pi}\int_r^R \frac{dI(x)}{dx}\frac{dx}{\sqrt{x^2 - r^2}} \tag{15}$$

$$I(x) = 2\int_0^{(R^2-x^2)^{1/2}} f(x)\,dx = 2\int_x^R \frac{f(r)r\,dr}{\sqrt{r^2 - x^2}} \tag{16}$$

where R is the radius of the object. The transformation of $I(x)$ to $f(x)$ of Equation (16) is called Abel transformation.

Equation (16) can be converted into

$$f(r) = -\frac{1}{2\pi r}\frac{d}{dr}2\int_r^R \frac{I(x)x\,dx}{\sqrt{x^2 - r^2}} \tag{17}$$

Let us assume that the observed value $I(x)$ can be obtained discretely at $X_n = n\Delta$ ($\Delta = r/(n-1)$, $n = 0 \sim N$), i.e. $I(x = n\Delta) = I_n$. Abel transformation allows the estimation of $f(r)$ as f_k from observed sequential data $I_0, \ldots, I_N$ as follows

$$f_k = \frac{1}{\pi\Delta}\sum_{n=0}^{N} \beta_{kn} I_n \tag{18}$$

where β_{kn} is a function of k and n [11]. Thus, the electric field distribution for the axisymmetric electrode configuration can be calculated using Abel transformation by measuring the intensity of laser beam while shifted in parallel with the Y-axis at a constant intervals. Both ratios of transmitted light intensities were transformed by Abel transformation. Next, the dc and ac electric field components were calculated using Equations (11) to (14) for the transformed ratios of transmitted light intensities.

3.3. EXPERIMENTAL RESULTS

3.3.1. ELECTRIC FIELD DISTRIBUTION FOR PARALLEL-PLANE ELECTRODE

Figure 7 shows experimental results of the ratios of transmitted light intensities I_ω/I_{dc} and $I_{1\omega}^{45}/I_{dc}^{45}$ at the center position between the parallel-plane electrodes under dc voltage $V_{dc} = -10$ kV. The horizontal and the vertical axes represent, respectively, the distance X from the rotational axis of the electrodes and the ratio of transmitted light intensities. It is evident in this Figure that $I_{1\omega}/I_{dc}$ decreases as X increases, that is, as the measuring point departs farther away from the center of the electrodes. This is because the effective length through which the

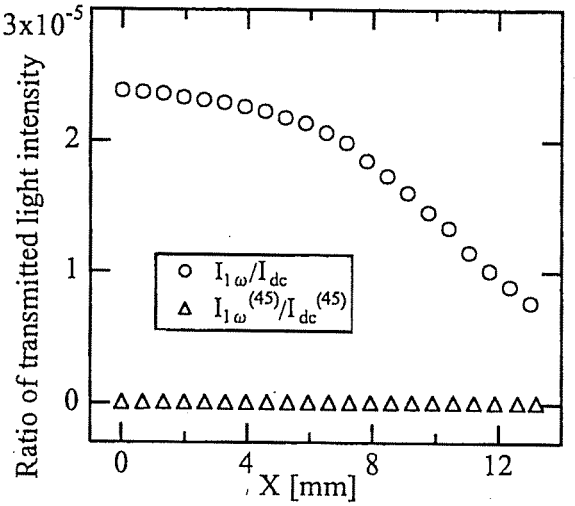

Figure 7. $I_{1\omega}/I_{dc}$ and $I_{1\omega}^{45}/I_{dc}^{45}$ as a function of position in the X direction (parallel-plane electrode configuration, $V_{dc} = -10$ kV, $V_{ac} = 200V_{peak}$, $d = 10$ mm).

phase shift is caused by Kerr effect decreases with an increase in X. On the other hand, as can be seen in Figure 7, $I_{1\omega}^{45}/I_{dc}^{45}$ is nearly zero irrespective of X.

Figures 8(a) and (b) shows, respectively, dc and ac electric field strength components E_{dc}, and E_{ac} and angles β_{dc} and β_{ac} as a function of X; these are calculated using Equation (11) to (14) after $I_{1\omega}/I_{dc}$ and $I_{1\omega}^{45}/I_{dc}^{45}$ shown in Figure 6 were transformed by Abel transformation. In these Figures, the solid and open circles represent measurement values of E_{dc} and E_{ac}, respectively. A solid line in Figure 8(a) represents a theoretically derived electric field profile for the parallel-plane electrode configuration using the charge simulation method. Note that both of the theoretical values of β_{dc} and β_{ac} are 90°. Hence, it is clear in Figures 8(a) and (b) that the theoretical and measured values agree very well each other. Consequently, it was confirmed from the experimental results that Equations (11) to (14) are applicable to the axisymmetric 3-dimensional electric field distribution measurements to obtain the magnitude and angle of the electric field vector independently.

3.3.2. ELECTRIC FIELD DISTRIBUTION FOR SPHERE-PLANE ELECTRODE

As an example of quasi-uniform field, we measured electric field distribution for the sphere-plane electrode configuration. Figure 9 shows experimental results of dc and ac field distributions near the plane electrode for $V_{dc} = -10$ kV. In Figure 9(a), the dc field strength E_{dc}, is slightly larger than the theoretical value in the region near $X = 0$, *i.e.* near the center of the plane electrode. The discrepancy can be explained as follows. In general, Abel transformation takes into account the contribution only inside a fictitious cylinder with a radius of R; we have assumed during the course of calculation that the electric field is ideally zero outside the cylinder. Since the actual electric field can exist even outside the cylinder, the laser beam undergoes more phase shift due to the Kerr effect. As a result, the measured E_{dc} becomes larger than the theoretical ones near $X = 0$. On the other hand,

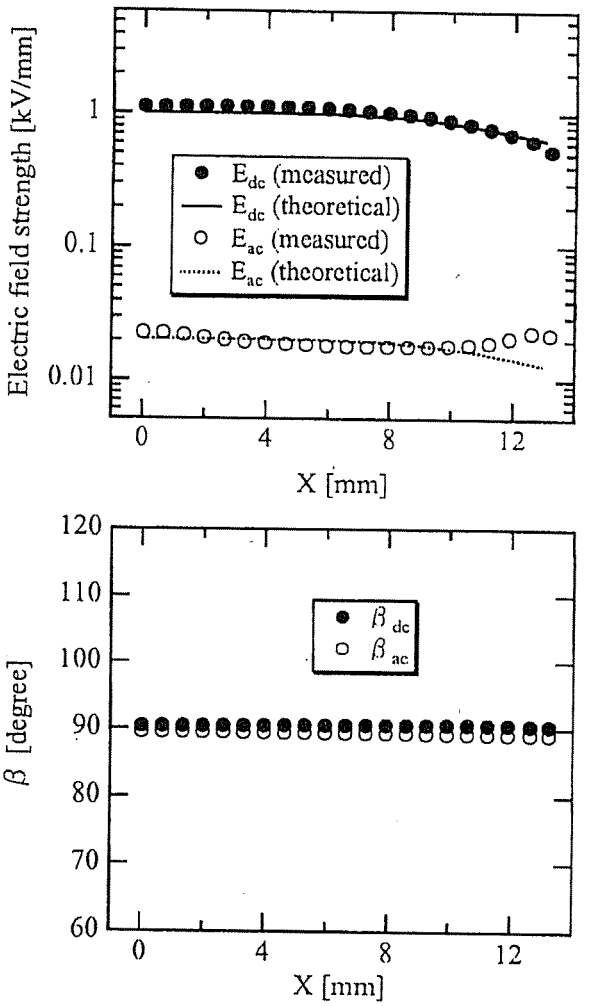

Figure 8. Measured electric field distribution in X direction (parallel-plane electrode configuration, $V_{dc} = -10$ kV, $V_{ac} = 200V_{peak}$, $d = 10$ mm). (a) E_{dc}, E_{ac} and (b) β_{dc}, β_{ac}.

E_{dc} is smaller than the theoretical curve at $X > 10$, *i.e.* near the edge of the electrode. We interpret the difference as follows: the effective path length is too short and the electric field strength is too small near the edge to measure E_{dc} with high sensitivity. Such a discrepancy arising from these factors for the electric field measurement should be further investigated.

4. CONCLUSIONS

We measured the 3-dimensional electric field distribution in a liquid dielectric with an axisymmetric electrode configuration using the Kerr electro-optic effect when an electric field vector was perpendicular to the laser beam direction. We derived the theoretical relations between the electric field vector and the ratio of transmitted light intensities for high sensitivity measurement system using a technique combined with ac field modulation and circular polarized light. Note that the above relations are applicable only if the electric field magnitude and direction are

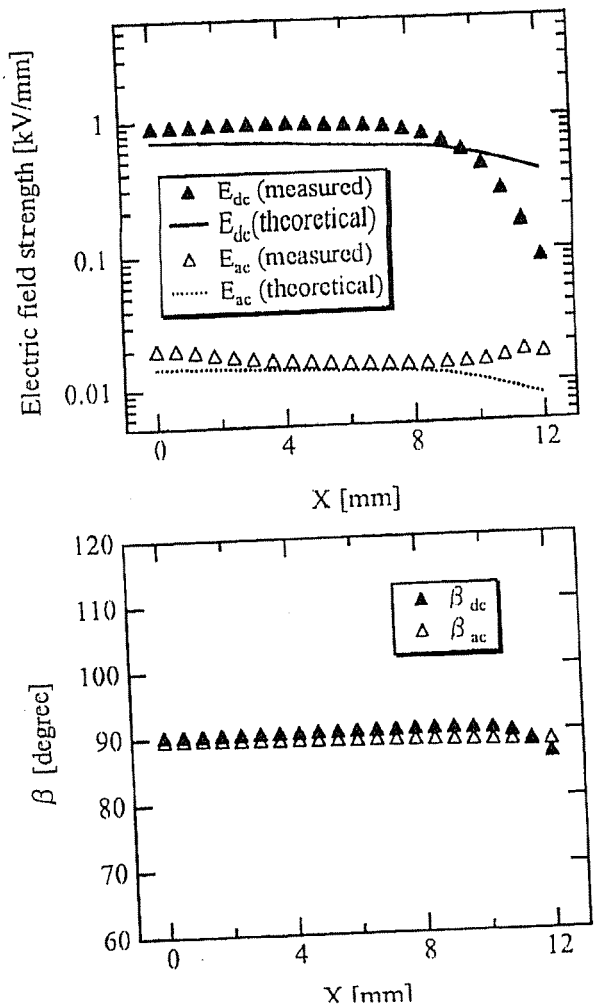

Figure 9. Measured electric field distribution in the X direction (sphere-plane electrode configuration, $V_{dc} = -10$ kV, $V_{ac} = 200V_{peak}$, $d = 10$ mm). (a) E_{dc}, E_{ac} and (b) β_{dc}, β_{ac}.

constant along the light path. The derived equations were verified experimentally for the electric field measurement in transformer oil with axisymmetric electrode configurations (parallel-plane, sphere-plane), *i.e.* measured electric field vectors proved to agreed well with the theoretical ones.

REFERENCES

[1] T. Maeno and T. Takada, "Electric Field Measurement in Liquid Dielectrics Using Combination of ac Voltage Modulation and a Small Retardation Angle", IEEE Trans. EI. Vol. 22, pp. 503–508, 1987.

[2] M. Hikita, M. Matsuoka, K. Kato, N. Hayakawa and H. Okubo, "Kerr Electrooptic Field Mapping in Transformer Oil/PET Film Composite Insulation System for dc Voltage Application", 4th ICPADM, pp. 71–74, 1994.

[3] M. Matsuoka, R. Shimizu, K. Kato, N. Hayakawa, M. Hikita and H. Okubo, "Influence of Impurity on Electric Field Distribution in Transformer Oil", 3rd Japan-Korea Symposium on Electrical Insulation and Dielectric Materials, pp. 47–50, 1994.

[4] U. Gäfvert, A. Jaksts, C. Törnkvist and L. Walfridsson, "Electrical Field Distribution in Transformer Oil", IEEE Trans. EI., Vol. 27, No. 3, pp. 647–660, 1992.

[5] Z. Peng, H. Xie and C. Zhang, "A New Kerr Electro-optic System for the Measurements of Electric Field and Space Charge Distribution", 4th ICPADM, pp. 674–677, 1994.

[6] S. Sumiyositani, "Theoretical Investigation on Kerr Electro-optic Measurement Method for Non-uniform Three-dimensional Electric Field", 4th ICPADM, pp. 705–708, 1994.

[7] M. Zahn and R. Hanaoka, "Kerr Eiectro-optic Measurements of Transformer Oil in a Point Plane Geometry", 4th ICPADM, pp. 697–700, 1994.

[8] M. Zahn, "Transform Relationship Between Kerr-effect Optical Phase Shift and Nonuniform Electric Field Distributions", IEEE Trans. on Dielectrics EI, Vol. 1, No. 2, pp. 235–246, 1994.

[9] K. Arii, H. Ihori, I. Takechi, S. Uto and I. Kitani, "Measurements of Three Dimensional Electric Field Distribution in Dielectric Liquids", 4th ICPADM, pp. 13–16, 1994.

[10] K. Tanaka and T. Takada, "Measurement of the 2-Dimensional Electric Field Vector in Dielectric Liquids", IEEE. Trans. Dielectrics EI., Vol. 1, No. 4, pp. 747–753, 1994.

[11] W. L. Barr, "Method for Computing the Radial Distribution of Emitters in a Cylindrical Source", Journal of the Optical Society of America, Vol. 52, No. 8, pp. 885–888, 1962.

Manuscript was received on 1 June 1995, in final form 12 January 1996.